Published in final edited form as:
J Am Chem Soc. 2012 February 1; 134(4): 1996–1999. doi:10.1021/ja210957u.

Preparation and Properties of a Monomeric High-Spin Mn^{V}–Oxo Complex

Taketo Taguchi[†], **Rupal Gupta**[‡], **Benedikt Lassalle-Kaiser**[¶], **David W. Boyce**[¥], **Vittal K. Yachandra**[¶], **William B. Tolman**[¥,*], **Junko Yano**[¶,*], **Michael P. Hendrich**[‡,*], and **A.S. Borovik**[†,*]

[†]Department of Chemistry, University of California-Irvine, 1102 Natural Sciences II, Irvine, CA 92697

[‡]Department of Chemistry, Carnegie Mellon University, Pittsburgh, PA 15213

[¶]Physical Biosciences Division, Lawrence Berkeley National Laboratory, Berkeley, CA 94720

[¥]Department of Chemistry and Center for Metals in Biocatalysis, University of Minnesota, Minneapolis, MN 55455

Abstract

Oxomanganese(V) species have been implicated in a variety of biological and synthetic processes, including as a key reactive center within the oxygen-evolving complex in photosynthesis. Nearly all mononuclear Mn^{V}–oxo complexes have tetragonal symmetry, producing low-spin species. A new Mn^{V}–oxo complex that is high-spin is now reported, which was prepared from a well-characterized oxomanganese(III) complex having trigonal symmetry. Titration experiments with $[FeCp_2]^+$ were monitored with optical and electron paramagnetic resonance (EPR) spectroscopies and support a high-spin oxomanganese(V) complex formulation. The parallel-mode EPR spectrum has a distinctive $S = 1$ signal at $g = 4.01$ with a six-line hyperfine pattern having $A_z = 113$ MHz. The presence of an oxo ligand was supported by resonance Raman spectroscopy, which revealed O-isotope sensitive peaks at 737 cm^{-1} and 754 cm^{-1} assigned as a Fermi doublet centered at 746 cm^{-1}($\Delta^{18}O = 31$ cm^{-1}). Kβ Mn X-ray emission spectra showed Kβ' and $K\beta_{1,3}$ bands at 6475.92 and 6490.50 eV, which are characteristic of a high-spin Mn^{V} center.

Manganese-oxo complexes have prominent roles in several chemical and biological processes.[1] In biology, high valent Mn–oxo species may be consequential in the oxidation of water to dioxygen within the photosynthetic membrane protein (Photosystem II, PSII).[2] Catalysis occurs at the oxygen-evolving complex (OEC) in PSII, which contains a Mn_4Ca cluster surrounded by a network of H-bonds. The structure of the cluster can be described as a Mn_3CaO_4 distorted cube with an oxo-bridged external manganese center. [3] The mechanism of water oxidation is still debated, yet one common proposal invokes the generation of high valent Mn species prior to the formation of the O-O bond.[4] In this premise, photo-oxidation would produce a high-energy transient state (S_4) containing Mn^{V}–oxo and Ca^{II}–OH centers that initially couple to form a peroxo intermediate and, ultimately, dioxygen (Figure 1).

*Corresponding Author*aborovik@uci.edu.

ASSOCIATED CONTENT

Experimental details for all chemical reactions and measurements, and figures for comproportionation reactions and electrochemical experiments. This material is available free of charge via the Internet at (http://pubs.acs.org/page/jacsat/submission/authors.html).

The properties of a Mn^{V}–oxo center that can lead to O–O bond formation are unknown, leading to efforts to prepare synthetic systems that probe this process. Some successes have been reported, including the work of Nam and Åkermark, [5] who showed that dioxygen can be produced from Mn(V)–O species and hydroxide ions. In addition to water oxidation, Mn^{V}–oxo complexes have been invoked as oxiddants in O-atom transfer reactions and C–H bond function-alization. [6] Most of these complexes contain ancillary porphyrin, [7] corrole,[8] corrolazine,[9] or salen ligands,[10] producing species that are low-spin with $S = 0$ spin ground states. This observation follows from the established theory that predicts that *all* tetragonal d^2 metal-oxo complexes will be diamagnetic, resulting in a triple bond between the metal center and the terminal oxo ligand (Figure 2A).[11] Results from the few characterized tetragonal Mn^{V}–oxo species support this prediction, insofar as the observed spectroscopic and structural properties indicate the existence of an $S = 0$ Mn≡O unit.[12]

The lone Mn^{V}–oxo site in the OEC could also be high spin ($S = 1$). Less is known about the chemistry of metal–oxo complexes in this spin state: we are aware of only one report concerning a high-spin Mn^{V}–oxo complex, a Mn^{V}(O)porphyrin species for which only a room temperature magnetic moment was used to evaluate its magnetic properties.[13] In addition, an isoelectronic Mn^{V} –imido complex has been prepared,[14] the properties of which suggested that it is paramagnetic. One approach toward preparing high-spin metal-oxo species is to enforce local trigonal symmetry within the complex. Mayer and Thorn[15] were the first to suggest that metal–oxo complexes with trigonal symmetry possess two low-lying degenerate orbitals that will produce $S = 1$ spin ground states for a d^2 metal-oxo complex (Figure 2B).[16] This theoretical prediction suggests that the metal–oxo interactions in such complexes are weaker compared to those with tetragonal symmetry, making the former a more reactive species.

This report describes the preparation and spectroscopic properties of a high-spin Mn^{V}–oxo complex, in which the oxo ligand arises from H_2O. The complex is supported by the ligand $[H_3buea]^{3-}$, which promotes C_3 molecular symmetry and influences the secondary coordination sphere through an intramolecular H-bonding network around the Mn^{V}–oxo unit. Our findings demonstrate the feasibility of high-spin Mn^{V}–oxo complexes and provide a spectroscopic framework for probing their role in chemical processes.

We have previously synthesized $[Mn^{III}H_3buea(O)]^{2-}$, the only example of a monomeric Mn^{III}–oxo complex (Figure 2C).[17] Unlike most monomeric metal-oxo complexes, there are three intramolecular H-bonds between the oxo ligand and $[H_3buea]^{3-}$ which aids in the isolation of the complex. $[Mn^{III}H_3buea(O)]^{2-}$ has unusually low oxidation potentials because of the highly anionic ligand field surrounding the manganese center, making it a convenient synthon to prepare higher valent Mn–oxo species. We showed that the one-electron oxidation of $[Mn^{III}H_3buea(O)]^{2-}$ to its Mn^{IV}–oxo derivative at room temperature in DMSO can be accomplished at −1.0 V vs $[FeCp_2]^{+/0}$ (−0.34 V vs NHE).[18] A second oxidative process was observed at −0.076 V vs $[FeCp_2]^{+/0}$ (+0.59 V vs NHE), which we assigned to the $Mn^{V/IV}$–oxo redox couple. However, this process was only reversible under the relatively fast scan velocity of 50 V/s, which hindered further characterization of this oxidized species at room temperature. We have found that measuring the redox potential at −60°C in 1:1 THF/DMF produced a quasi-reversible one-electron redox process at −0.08 V vs $[FeCp_2]^{+/0}$ at significantly slower scan velocities of 0.100 V/s (Figure S1), suggesting the possibility for detecting this putative Mn^{V}–oxo species at lower temperatures.

The sequential oxidation of $[Mn^{III}H_3buea(O)]^{2-}$ was followed spectrophotometrically at −80°C in a DMF/THF solution (Scheme 1, Figure 3A). The optical properties of $[Mn^{III}H_3buea(O)]^{2-}$ at λ_{max} = 710 and 500 nm disappear upon the addition of 1 equiv of $[FeCp_2]^{+}$ to produce a spectrum with bands at λ_{max} = 640 and 420 nm. These features are

identical to those obtained for $[Mn^{IV}H_3buea(O)]^-$ when measured at room temperature in DMSO.[18a] Treating the solution with another equivalent of $[FeCp_2]^+$ caused a new spectrum to appear, containing peaks at λ_{max}, nm (ε_M)= 820 (3600), 620 (3400) and 430 (10,000), which persists for hours at −80°C. We assign these features to the Mn^V–oxo complex, $[Mn^VH_3buea(O)]$.

The oxidation of $[Mn^{III}H_3buea(O)]^{2-}$ by $[FeCp_2]^+$ was also studied using parallel (∥) and perpendicular (⊥) mode EPR spectroscopy. We found that $[Mn^{III}H_3buea(O)]^{2-}$ has no signals in ⊥-mode but shows a 6-line hyperfine pattern (A_z = 280 MHz, 10 mT) in ∥-mode at g = 8.08 (Figure 4A), which is indicative of an S = 2 spin state.[19] One-electron oxidation of $[Mn^{III}H_3buea(O)]^{2-}$ was evident by the loss of the g = 8.08 signal in the ∥-mode EPR spectrum and the appearance of features at g = 5.26, 2.38 and 1.62 in the ⊥-mode spectrum (Figure 4B). These signals are associated with $[Mn^{IV}H_3buea(O)]^-$ as reported previously.[18a] The relative signal intensities of $[Mn^{III}H_3buea(O)]^{2-}$ and the simulations of the Mn^{IV}-oxo showed that 80% of the manganese in the sample was converted to $[Mn^{IV}H_3buea(O)]^-$. The 11-line hyperfine pattern centered at g = 2 is proposed to originate from a minority mixed-valent species (< 1% in manganese).

Further oxidation of the sample produced a new signal in ∥-mode centered at g = 4.01 (Figure 4C),[20] which displayed a 6-line hyperfine splitting of 113 MHz (4 mT) (Figure 3B). The position of the signal is indicative of a transition from the $|1^{\pm}>$ doublet of an S = 1 spin manifold,[20,21] and, taken together with the hyperfine splitting, is consistent with a monomeric Mn^V species that is assigned to $[Mn^VH_3buea(O)]$. Simulations of this signal indicated that 60% of the initial Mn^{III}–oxo species was converted to $[Mn^VH_3buea(O)]$.

Additional support for the S = 1 spin state for $[Mn^VH_3buea(O)]$ came from Kβ manganese X-ray emission spectroscopy (XES). Figure 5 shows the Mn Kβ emission spectrum of $[Mn^VH_3buea(O)]$ and of the low-spin oxomanganese(V) complex $[Mn^VDMB(O)]^-$,[12b] recorded at 10 K. The low-spin oxomanganese(V) shows a single peak ($K\beta_{1,3}$) at 6489.06 eV, while the spectrum of $[Mn^VH_3buea(O)]$ is split into two peaks, $K\beta_{1,3}$ at 6490.50 eV and its satellite peak (Kβ') at ~6476 eV. The $K\beta_{1,3}$ peak of $[Mn^VH_3buea(O)]$ is shifted to higher energy by 1.44 eV compared to that of $[Mn^VDMB(O)]^-$.

$K\beta_{1,3}$ XES detects the X-ray emission from the relaxation of a 3*p* electron to a 1*s* hole, which is created by excitation of an 1*s* electron. The energy splitting in Kβ spectra is caused by the exchange interaction between 3*p* and 3*d* orbitals. [22] Two final states ($K\beta_{1,3}$ and Kβ') exist because of constructive ($K\beta_{1,3}$) or destructive (Kβ') spin-exchange interactions between the unpaired electrons in the 3*p* and 3*d* orbitals (Figure 5B). The Kβ spectrum is thus sensitive to the effective number of unpaired 3*d* electrons and has been used to determine the Mn oxidation states in synthetic complexes and the OEC.[23] Splitting of $K\beta_{1,3}$ peak has been observed previously between low- and high-spin Fe^{III} species: [24] a shift of ~ 0.7 eV for the $K\beta_{1,3}$ peak position was found between the low- and high-spin species. For the low-spin complex, the Kβ' peak moved towards and merged into the low energy side of the $K\beta_{1,3}$ line because of a decrease in valence spin. Analogous trends were observed in the Kβ XES spectra of $[Mn^VH_3buea(O)]$ and $[Mn^VDMB(O)]^-$, findings that are consistent with $[Mn^VH_3buea(O)]$ having an S = 1 spin ground state.

In order to confirm the presence of the oxo ligand in $[Mn^VH_3buea(O)]$, resonance Raman (rR) spectroscopy was performed (λ_{ex} = 647.1 nm, 77 K). The rR spectrum of $[Mn^VH_3buea(^{16}O)]$ contained oxygen-sensitive features at 737 cm^{-1} and 754 cm^{-1} that converted to a single feature at 715 cm^{-1} when the sample was prepared with H_2 ^{18}O (Figure 6). On the basis of this behavior, and the fact that none of the peaks were observed in rR spectra of the Mn^{III} or Mn^{IV} precursors,[25] we postulate that the two peaks in the ^{16}O

sample comprise a Fermi doublet, a relatively common phenomenon in metal-oxygen compounds.[26] In support of assigning these features to a Mn^{V}-O vibration, the observed difference of 31 cm^{-1} between the average position of the two peaks in the ^{16}O sample (746 cm^{-1}) and the 715 cm^{-1} peak in the ^{18}O sample agrees with the value expected based on a harmonic Mn—O oscillator ($\nu(Mn–^{16}O)/\nu(Mn–^{18}O)$ = 1.043; calc'd = 1.046). The Mn^{V}–O vibration occurs at a slightly higher energy than that found by FTIR spectroscopy for $[Mn^{IV}H_3buea(O)]$ (ν(Mn–O) = 737 cm^{-1}),[18a] which is consistent with the electron being removed from orbitals not involved in Mn–O bonding (Figure 2B). The Mn–O vibration observed for $[Mn^{V}H_3buea(O)]$ is similar to the ν(Mn–O) of 759 cm^{-1} reported for a 6-coordinate Mn^{V}–oxo porphyrin complex; however, it is at significantly lower energy than those reported for nonporphyrinic low-spin oxomanganese(V) complexes. For example, the low-spin $[Mn^{V}DMB(O)]^{-}$ complex has an Mn–O vibration of 973 cm^{-1}.[12b] This difference in vibrational energies reflects the disparate Mn–O bond orders predicted for high- and low-spin oxomanganese(V) complexes (Figure 2) and the likelihood that the Mn–O bond in $[Mn^{V}H_3buea(O)]$ forms intramolecular H-bonds with the $[H_3buea]^{3-}$ ligand.

With the characterization of $[Mn^{V}H_3buea(O)]$ we have now prepared oxomanganese complexes in three different oxidation levels, which have similar primary and secondary coordination spheres. The chemistry within this series of complexes is currently under investigation but preliminary results are consistent with our spectroscopic findings that all are monomeric oxomanganese species. For instance, treating the newly discovered $[Mn^{V}H_3buea(O)]$ complex with 1 equiv of $[Mn^{III}H_3buea(O)]^{2-}$ produced 2 equiv of $[Mn^{IV}H_3buea(O)]^{-}$ as determined by EPR and optical spectroscopies (Figure S2). This reaction is consistent with the comproportionation reaction described by eq 1

$$[Mn^{V}H_3buea(O)]+[Mn^{III}H_3buea(O)]^{2-} \xrightarrow[-80°C]{THF/DMF} 2[Mn^{IV}H_3buea(O)]^{-} \quad (1)$$

Our work has further shown that changes in spin state within the series can be monitored with EPR spectroscopy, illustrating the utility of using ǁ-mode methods to probe integer-spin states. In addition, we have obtained the first high-spin manganese(V) EPR and XES spectra that can now be used as references in the study of other high valent manganese systems, such as those that may be present in the OEC of PSII. These results also establish the viability of high-spin oxomanganese(V) species as possible reactive intermediates in a variety of chemical processes.

Supplementary Material

Refer to Web version on PubMed Central for supplementary material.

Acknowledgments

We thank Drs. J. Kern, R. A. Mori, and T.-C. Weng for their help during the XES data collection and Professor T. J. Collins for providing $[NEt_4][Mn^{V}DMB(O)]$.

Funding Sources

The authors thank the NIH (GM50781 to ASB; GM77387 to MPH; GM47365 to WBT; and GM55302 to VKY)) and the Office of Science, Basic Energy Sciences (BES), Division of Chemical Sciences, Geosciences and Biosciences, Department of Energy under Contract No. DE-AC02-05CH11231 (VKY and JY) for financial support. Portions of this research were carried out at Stanford Synchrotron Radiation Lightsource (SSRL) operated by DOE, OBES.

ABBREVIATIONS

$[H_3buea]^{3-}$ tris[(*N*-*tert*-butylureaylato)-*N*-ethylene]aminato

DMB is a tetra-amido marcocylic ligand

REFERENCES

1. (a) Groves, JT.; Han, YZ. Cytochrome P-450. Structure, Mechanism and Biochemistry. Ortiz de Montellano, RR., editor. New York: Plenum Press; 1995. p. 3-48.(b) Holm RH. Chem. Rev. 1987; 87:1401–1449.(c) Gardner KA, Kuehnert LL, Mayer JM. Inorg. Chem. 1997; 36:2069–2078. [PubMed: 11669825]
2. Meyer TJ, Nuynh MHV, Thorp HH. Angew. Chem. Int. Ed. 2007; 46:5284–5304.
3. Umena Y, Kawakami K, Shen J-R, Kamiya N. Nature. 2011; 473:55–60. [PubMed: 21499260]
4. (a) McEvoy JP, Brudvig GW. Chem. Rev. 2006; 106:4455–4483. [PubMed: 17091926] (b) Cady CW, Crabtree RH, Brudvig GW. Coord. Chem. Rev. 2008; 252:444–455. [PubMed: 21037800]
5. (a) Kim SH, Park H, Seo MS, Kubo M, Ogura T, Klajn J, Gryko DT, Valentine JS, Nam W. J. Am. Chem. Soc. 2010; 132:14030–14032. [PubMed: 20845972] (b) Gao Y, Akermark T, Liu J, Sun L, Akermark B. J. Am. Chem. Soc. 2009; 131:8726–8727. [PubMed: 19496534]
6. Groves JT, Lee J, Marla SS. J. Am. Chem. Soc. 1997; 119:6269–6273.
7. (a) Jin N, Groves JT. J. Am. Chem. Soc. 1999; 121:2923–2924.(b) Song WJ, Seo MS, George SD, Ohta T, Song R, Kang M-J, Tosha T, Kitagawa T, Solomon EI, Nam W. J. Am. Chem. Soc. 2007; 129:1268–1277. [PubMed: 17263410]
8. Gross Z, Golubkov G, Simkhovich L. Angew. Chem. Int. Ed. 2000; 39:4045–4047.
9. Prokop KA, de Visser SP, Goldberg DP. Angew. Chem. Int. Ed. 2010; 49:5091–5095.
10. Jacobsen EN, Zhang W, Muci AR, Ecker JR, Deng L. J. Am. Chem. Soc. 1991; 113:7063–7064.
11. (a) Ballhausen CJ, Gray HB. Inorg. Chem. 1962; 1:111–122.(b) Mayer JM. Comm. Inorg. Chem. 1988; 8:125–135.(c) Winkler JR, Gray HB. Struct. Bond. 2011 ASAP.
12. (a) Collins TJ, Powell RD, Slebonick C, Uffelman ES. J. Am. Chem. Soc. 1990; 112:899–901.(b) Workman JM, Powell RD, Procyk AD, Collin TJ, Bosian DF. Inorg. Chem. 1992; 31:1548–1550. (c) Lansky DE, Mandimutsira B, Ramdhanie B, Clausen M, Penner-Hahn J, Zvyagin SA, Telser J, Krzystek J, Zhan R, Ou Z, Kadish KM, Zakharov L, Rheingold AL, Goldberg DP. Inorg. Chem. 2005; 44:4485–4498. [PubMed: 15962955]
13. Groves JT, Kruper WJ, Haushalter RC. J. Am. Chem. Soc. 1980; 102:6375–6377.
14. Zdilla MJ, Dexheimer JL, Abu-Omar MM. J. Am. Chem. Soc. 2007; 129:11505–11511. [PubMed: 17718564]
15. Mayer JM, Thorn DL, Tulip TH. J. Am. Chem. Soc. 1985; 107:7454–7462.
16. For examples of high-spin oxochromiun(IV) complexes see: Hess A, Hörz MR, Liable-Sands LM, Lindner DC, Rheingold AL, Theopold KH. Angew. Chem. Int. Ed. 1999; 38:166–168. Qin K, Incarvito CD, Rheingold AL, Theopold KH. J. Am. Chem. Soc. 2002; 124:14008–14009. [PubMed: 12440895]
17. Borovik AS. Acc. Chem. Res. 2005; 38:54–61. [PubMed: 15654737]
18. (a) Parsell TH, Behan RK, Hendrich MP, Green MT, Borovik AS. J. Am. Chem. Soc. 2006; 128:8728–8729. [PubMed: 16819856] (b) Parsell TH, Yang M-Y, Borovik AS. J. Am. Chem. Soc. 2009; 131:2762–2763. [PubMed: 19196005]
19. Hendrich MP, Debunner P. Biophys. J. 1989; 56:489–506. [PubMed: 2551404]
20. A total of 3 equiv of $[FeCp_2]^+$was used to ensure complete oxidation at −80°C (see Figure 4C).
21. Details of this spectrum will be discussed in a forthcoming report.
22. (a) Tsutsumi K, Nakamori H, Ichikawa K. Phys. Rev. B: Condens. Matter. 1976; 13:929–933.(b) Thole BT, Cowan RD, Sawatzky GA, Fink J, Fuggle JC. Phys. Rev. B. 1985; 31:6856–6858.
23. (a) Messinger J, Robblee JH, Bergmann U, Fernandez C, Glatzel P, Visser H, Cinco RM, McFarlane KL, Bellacchio E, Pizarro SA, Cramer SP, Sauer K, Klein MP, Yachandra VK. J. Am.

Chem. Soc. 2001; 123:7804–7820. [PubMed: 11493054] (b) Glatzel P, Bergmann U. Coord. Chem. Rev. 2005; 249:65–95.

24. Wang X, Randall CR, Peng G, Cramer SP. Chem. Phys. Lett. 1995; 243:469–473.
25. O-sensitive peaks were not observed in rRaman spectra for independently prepared samples of $[Mn^{III}H_3buea(O)]^{\square}$ and $[Mn^{IV}H_3buea(O)]^{-}$ that were collected under the same experimental conditions. Spectra were also collected for $[Mn^{IV}H_3buea(O)]^{-}$ with λ_{ex} = 457.9 and 488.0 nm and no O-isotope sensitive peaks were observed, indicating that the observed peaks in the rR spectra of the Mn^{V} species originated exclusively from $[Mn^{V}H_3buea(O)]$.
26. (a) Holland PL, Cramer CJ, Wilkinson EC, Mahapatra S, Rodgers KR, Itoh S, Taki M, Fukuzumi S, Que L Jr, Tolman WB. J. Am. Chem. Soc. 2000; 122:792–802.(b) Wilkinson EC, Dong Y, Zang Y, Fujii H, Fraczkiewicz R, Fraczkiewicz G, Czernuszewicz RS, Que L Jr. J. Am. Chem. Soc. 1998; 120:955–962.(c) Namuswe F, Hayashi T, Jiang Y, Kasper GD, Narducci Sarjeant AA, Moënne-Loccoz P, Goldberg DP. J. Am. Chem. Soc. 2010; 132:157–167. [PubMed: 20000711]

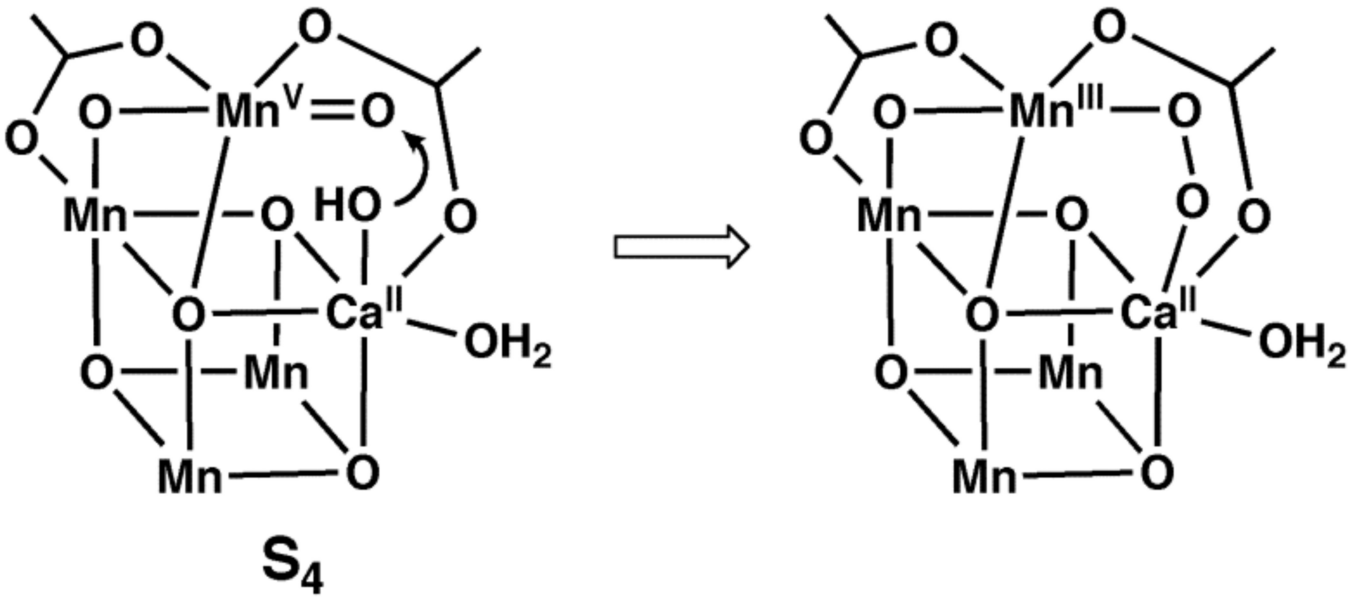

Figure 1.
Hypothetical representation of the S_4 state in the OEC and a possible route to the formation of the O–O bond.

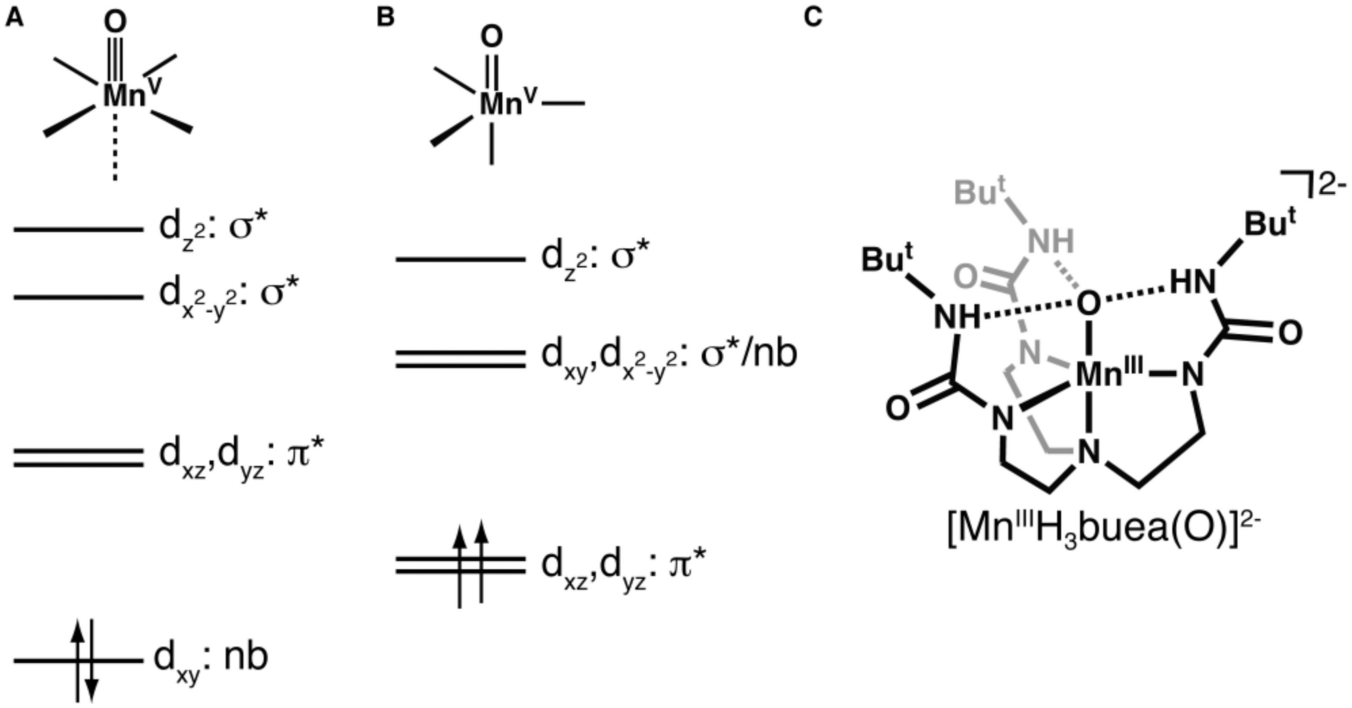

Figure 2.
Qualitative orbital splitting diagrams for oxometal complexes with (**A**) tetragonal[11a] and (**B**) trigonal[15] symmetries, and (**C**) the structure of the oxomanganese(III) precursor.

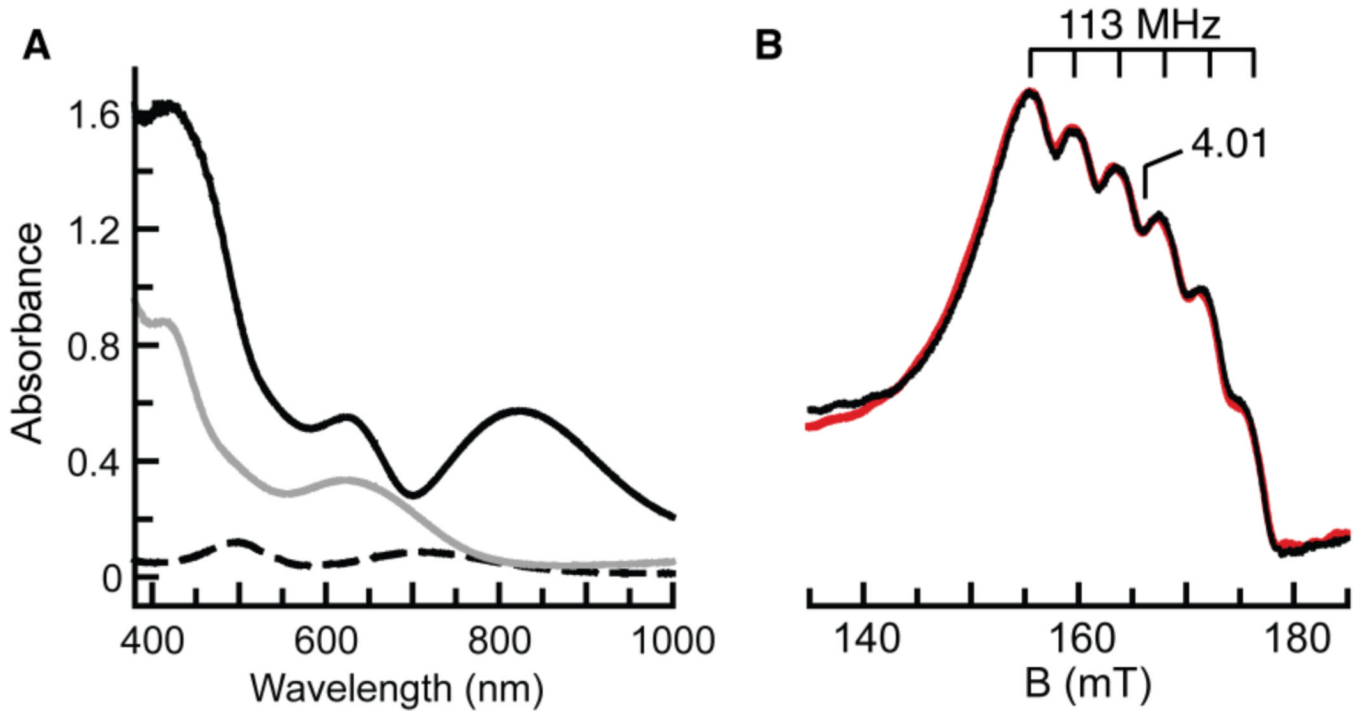

Figure 3.

(**A**) Electronic absorbance spectra of $[Mn^{I–II}H_3buea(O)]^{2-}$ (- - -), $[Mn^{IV}H_3buea(O)]^{-}$ (—), and $[Mn^{V}H_3buea(O)]$ (—) collected at −80°C in 1:1 THF/DMF. (**B**) ∥-mode EPR spectrum of $[Mn^{V}H_3buea(O)]$ (black) and simulated spectrum (red). See Figure 4 for experimental conditions.

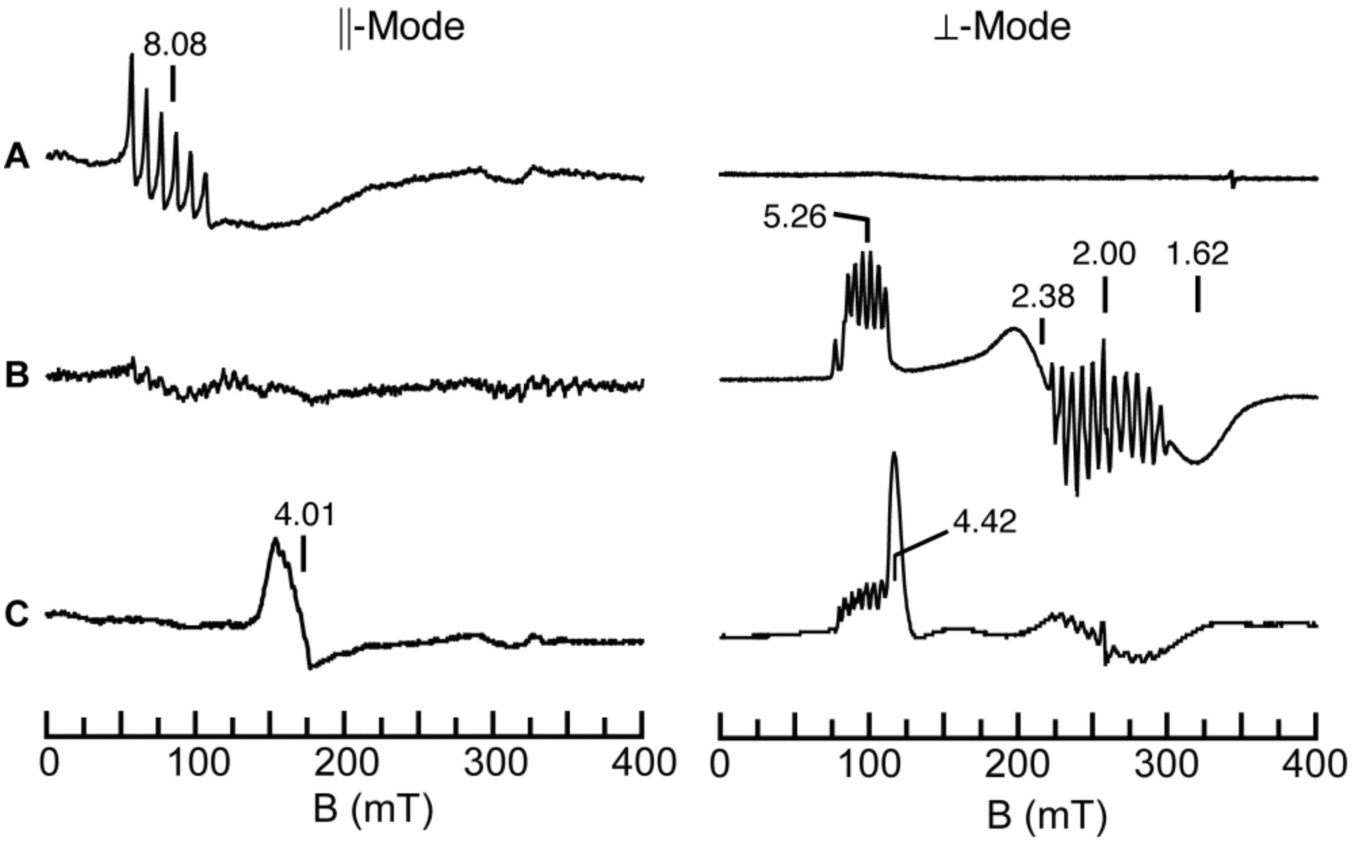

Figure 4.

∥- (left) and ⊥-mode (right) EPR spectra of a (**A**) $[Mn^{III}H_3buea(O)]^{2-}$); and after addition of approximately (**B**) one and (**C**) three equiv of $[FeCp_2]^+$. The peak at $g = 4.42$ in the ⊥-mode spectrum in C is from excess $[FeCp_2]^+$. Experimental conditions, temperature, 10 K; microwave frequency, 9.29 (∥) or 9.62 (⊥) GHz.

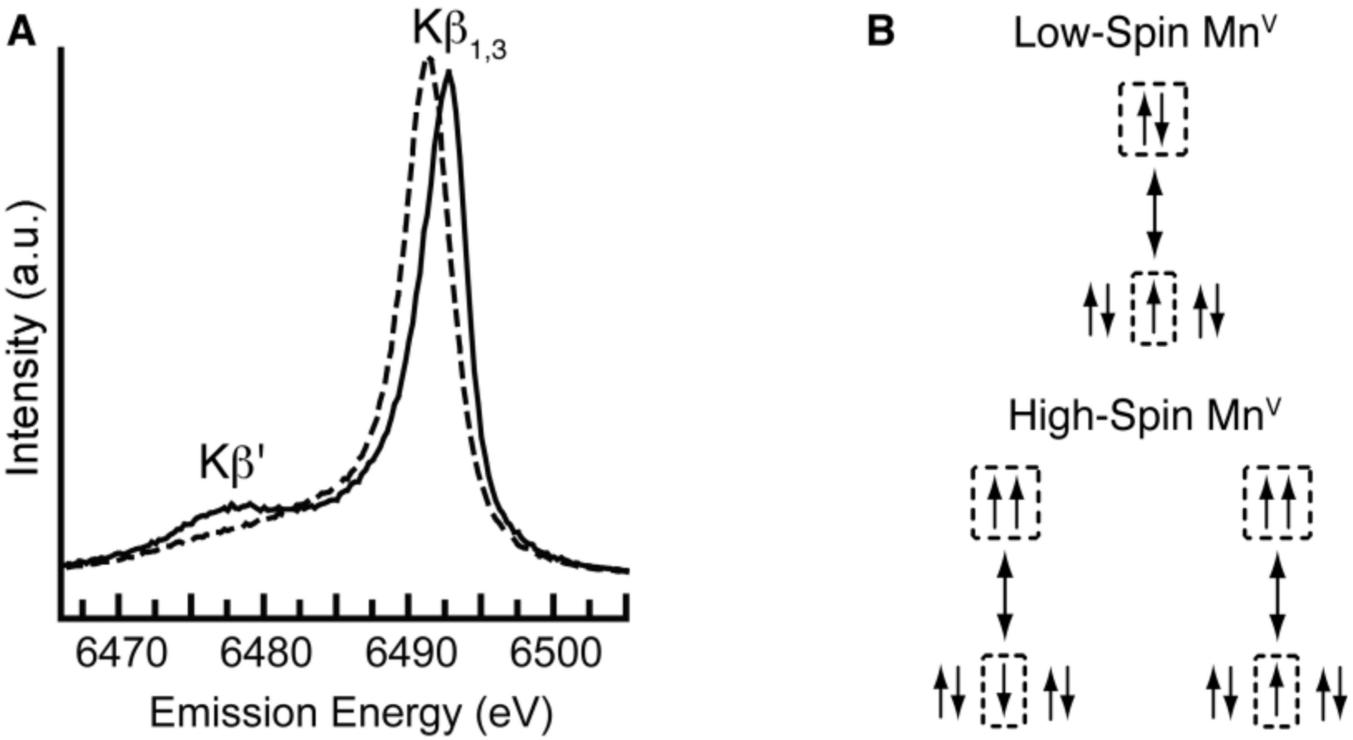

Figure 5.

(**A**) XES spectra of [$Mn^{V}H_3$buea(O)] (—) and the low-spin oxomanganese(V) complex [Mn^{V}DMB(O)] (- - -) collected at 10K with an excitation energy of 10.0 keV and (**B**) schematic diagrams of the 3*d*-3*p* exchange interactions in low- and high-spin Mn^{V} systems.

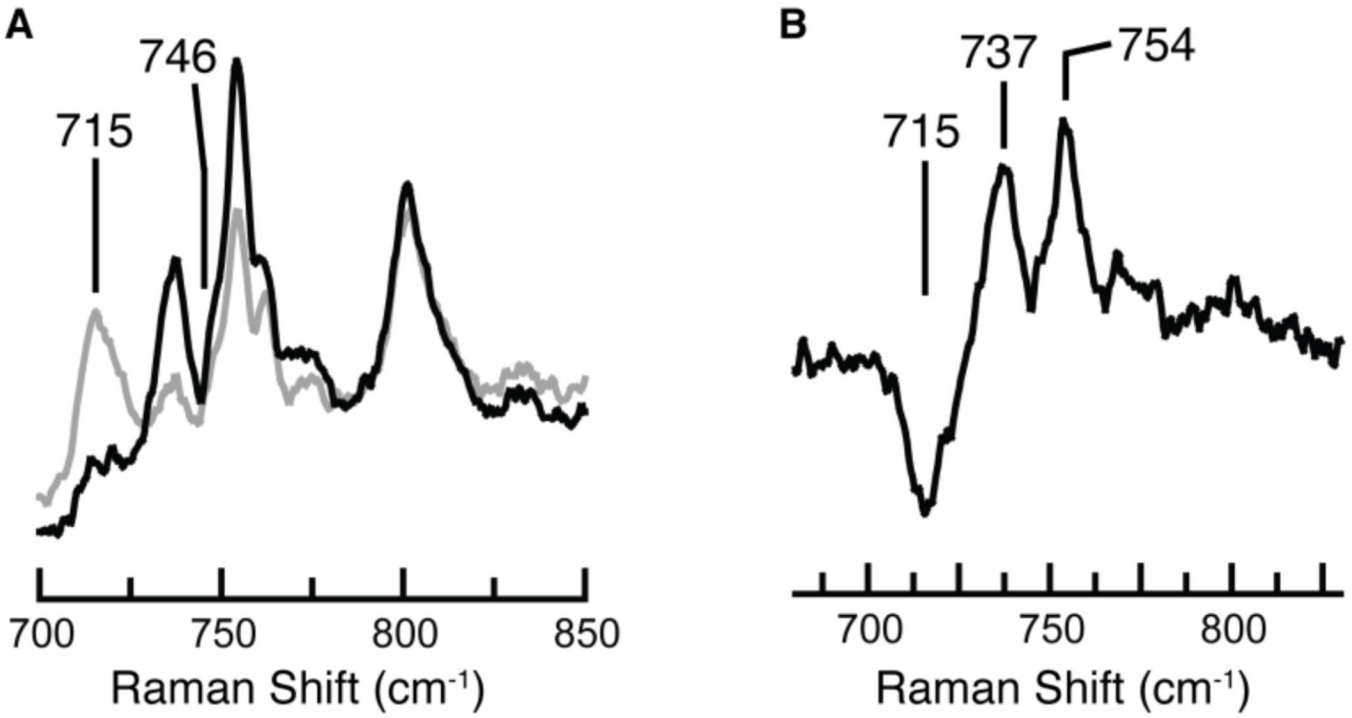

Figure 6.

Resonance Raman spectra of (**A**) [$Mn^{V}H_3buea(^{16}O)$] (black) and [$Mn^{V}H_3buea(^{18}O)$] (gray) collected at 77 K with λ_{ex} = 647.1 nm and (**B**) their difference spectrum ($^{16}O - ^{18}O$).

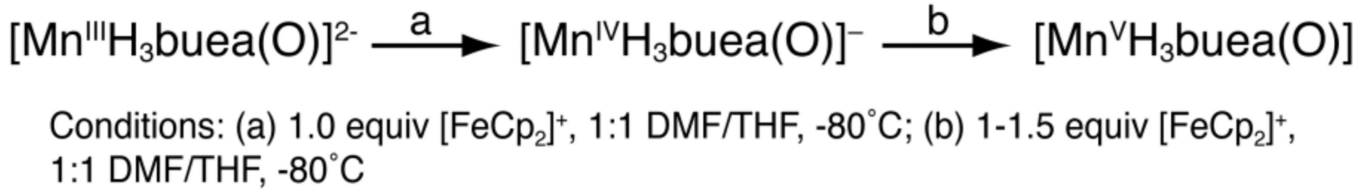

Scheme 1.
Conditions: (a) 1.0 equiv $[FeCp_2]^+$, 1:1 DMF/THF, −80°C; (b) 1–1.5 equiv $[FeCp_2]^+$, 1:1 DMF/THF, −80°C